

# EFFECTS OF PULSE DISTORTION ON PHASE VELOCITY MEASUREMENTS USING THE ZERO-CROSSING SHIFT TECHNIQUE

Y. Li and R. B. Thompson  
Ames Laboratory  
Iowa State University  
Ames, Iowa 50011

## INTRODUCTION

One of the technique that is often used in the measurement of phase velocities of guided elastic modes is the zero-crossing shift technique. Using this technique, one measures time delays (usually through a counter) of a specific zero-crossing for a number of different separation distances of two transducers. The phase velocity  $V_p$  is computed as the slope of the distance-delay plot. For non-dispersive waves, this produces no problem as the pulse retains its shape as it propagates.

For dispersive waves, however, things are more complicated because of pulse distortion. First of all, because the group velocity  $V_g$  and the phase velocity  $V_p$  are unequal, the position of a selected zero-crossing may move out of the pulse envelope when the change of transducer separation is large, making it hard to obtain a reliable phase velocity. Secondly, the pulse has many frequency components, and each frequency travels at a different velocity. The behavior of a particular zero crossing may not be characteristic of the phase velocity at a single frequency.

One of the applications of the zero-crossing shift technique is in the texture characterization of metal plates, where the texture induced anisotropy of plates is detected by the ultrasonic phase velocities [1]. These anisotropies are generally quite small, being on the order of a percent. To obtain good estimations of the texture parameters, the accuracy of the phase velocity measurement must be high. The commonly used transducers in texture characterization are electro-magnetic acoustic transducers (EMATs) which launch and pick up narrowband tonebursts. One of the waves used in texture characterization of plates is the  $S_0$  Lamb mode at around 500 KHz, which is known to have dispersions that are also on the order of a percent for plates of thicknesses on the order of a mm [2].

To understand and assess the effects of pulse distortion on phase velocity measurements using the zero-crossing technique, we will here establish a general pulse distortion model and use it to analyze the propagation of a Gaussian shaped pulse. Also to be presented and discussed are some computer simulation results from the model.

## THEORY AND MODEL

To investigate the pulse distortion phenomenon, Thompson and Elsley [3]

proposed the following model. Let us assume that only the  $S_0$  mode of propagation is present. Then a propagating wave may be described by the form

$$u(t, x) = \frac{1}{2\pi} \int_{-\infty}^{\infty} A(k) e^{j(\omega t - kx)} dk \quad (1)$$

where  $A(k)$  is a function relating to the bandwidth of  $k$ , i.e. the spatial frequencies excited by the transducer, and  $\omega$  is related to  $k$  by the dispersion relation.

The dispersion relation can be simplified by making a Taylor expansion at  $k=k_0$ :

$$\omega = \omega(k_0) + \omega'(k_0)(k-k_0) + \frac{1}{2} \omega''(k_0)(k-k_0)^2 + \dots \quad (2)$$

where  $(k_0, \omega_0)$  is the point of operation (center wave number and frequency)

$$\text{and } \omega'(k_0) = V_g \left. \frac{d\omega}{dk} \right|_{k=k_0} \text{ and } \omega''(k_0) = \left. \frac{d^2\omega}{dk^2} \right|_{k=k_0}.$$

For an arbitrary  $A(k)$ , numerical integration is usually required to evaluate  $u(t, x)$ . When  $A(k)$  is a Gaussian function, however, integration can be carried out analytically, and some physical insight can be obtained.

Let  $A(k) = B \exp\left\{-\frac{1}{2}(k-k_0)^2 B^2\right\}$ . Substituting this expression into (1) and carrying out the integration, leads to the relation

$$u(t, x) = |U(t, x)| \exp\{j[\omega_0 t - k_0 x + \text{Arg}(t, x)]\} \quad (3)$$

$$\text{with } |U(t, x)| = \frac{\exp\left\{-\frac{(V_g t - x)^2}{2B^2(1+a^2)}\right\}}{\sqrt{2\pi} (1+a^2)^{1/4}} \quad (3a)$$

$$\text{and } \text{Arg}(t, x) = \frac{1}{2} \tan^{-1} a - \frac{(V_g t - x)^2 a}{2B^2(1+a^2)} \quad (3b)$$

where  $a = \omega''(k_0) t/B^2$ .

Eqs. (3) show the following:

(1) At  $t=0$ , the wave has a Gaussian envelope in space. At  $x=0$ , the amplitude in time is not Gaussian, but it has a symmetric shape.

(2) For  $t > 0$ , the wave envelope retains its Gaussian shape in space, but changes amplitude and width.

(3) For  $x > 0$ , the Gaussian envelope in time becomes skewed as it propagates; i.e. not symmetric about the peak of the pulse. This is due to a time variable in the denominator part of exponentiation. The further the wave propagates, the more severe the skewing effect.

(4) The peak amplitude of the envelope moves at group velocity  $V_g = x/t$  as expected. The peak, however, does not remain at the center of the temporal envelope as the wave propagates, due to the distortion noted above.

(5) The pulse width increases as the wave propagates. It is readily seen that pulse width is proportional to  $\sqrt{1+a^2}$  or  $\sqrt{1+[\omega'' t/B^2]^2}$ . For a specific pulse propagating in a specific plate,  $a^2$  will eventually exceed 1.0 and become dominant. As can be seen in Eqs. (3), the pulse distortion and phase shift are

determined by the  $\omega''(k_0)$  term. Had this term vanished, there would be no pulse distortion and phase shift.

(6) The peak amplitude decreases even in the absence of attenuation. The rate of decrease is proportional to  $(1+a^2)^{1/4}$ .

(7) The presence of dispersion introduces an extra phase shift given by Eq. 3(b), such that linear relation of  $t$  and  $x$  no longer exists.

Figs. 1 and 2 show some experimental wave forms as well as simulated wave forms. The wave forms in Figs. 1 are obtained using two 1 MHz piezoelectric transducers on a 2.2 mm thick Al plate. The mode is  $S_0$  mode with the center frequency of 0.9 MHz. The simulated wave forms are obtained from Eqs. 3 and Eq. 4 (to be presented in next section). The parameters used are: thickness  $b=2.2$  mm; Poisson ratio  $\nu=0.345$ ; plane shear wave velocity  $V_t=3.10$  mm/ $\mu$ s; wave length  $D=5.0$  mm;  $B=7.5$  mm. These waves are not from current texture experiment; they have been selected to show the characteristics of dispersive waves. As will be shown later, the  $S_0$  wave in the current texture characterization experiment has a wider pulse width and is less dispersive.

In the above listed seven items, the first six do not really introduce any complication to the zero-crossing measurement technique. The last one, however, is of concern, since it destroys the linearity of the  $t$ - $x$  relation. In the

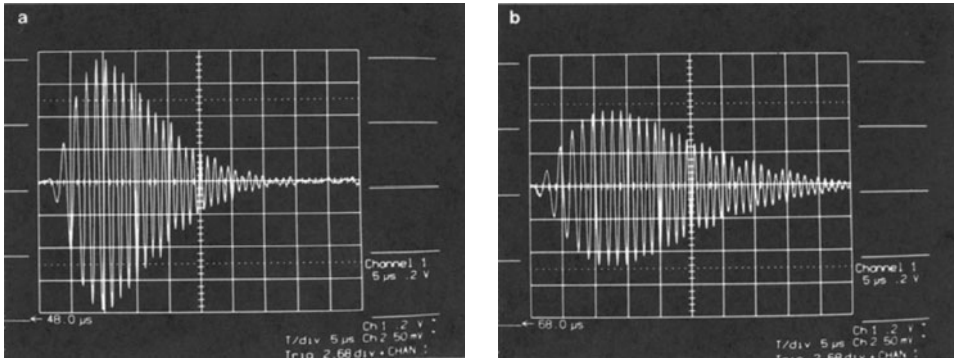


Fig.1. Experimental forms (a)  $x=150$  mm, (b)  $x=250$  mm

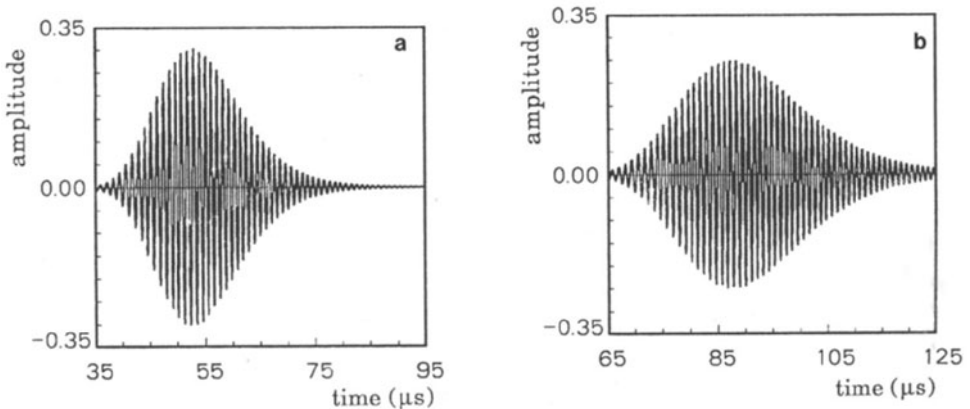


Fig.2. Simulated wave forms (a)  $x=150$  mm, (b)  $x=250$  mm

next section, we will investigate in depth the effects the phase shifting on the reliability of velocity measurement from the zero-crossing technique.

## SIMULATION

The model in above section is applicable to a general dispersion. Next, this model will be used to study quantitatively the influence of dispersion induced phase shifts on the velocity measurements of the  $S_0$  Lamb mode. We will use the experimental configuration at our laboratory as a simulation basis. Since texture characterization is performed in the low frequency region, the dispersion of  $S_0$  mode is relatively weak [2].

To perform the computer simulation, the functions  $\omega(k_0)$ ,  $\omega'(k_0)$ , and  $\omega''(k_0)$  must be obtained first. This involves solving the Rayleigh-Lamb dispersion equation and evaluating numerical derivatives. Thus, the computation required can be very extensive. Numerical studies in this section are based on a polynomial expression which closely approximates the corresponding isotropic dispersive equation.

The approximate dispersion relation to be used here is

$$W = \sqrt{2}K \left[ \sqrt{\frac{1}{1-\nu}} (1-4K^3+3K^4) + \frac{1}{2}K^3(1+K) + 4K^3(1-K) \right] \quad (4)$$

where  $W = \frac{b}{\pi} \frac{\omega}{v_t}$ ,  $K = \frac{b}{\pi} k$ , and  $\nu$  is the Poisson ratio of the plate material.  $v_t$  is the transverse plane wave velocity and  $k$  is the guided mode wave number.

Eq. (4) was developed by forcing a fifth degree polynomial satisfying the following boundary conditions:

$$W=0, \quad W' = dW/dK = \sqrt{2/(1-\nu)}, \quad W''=W'''=0 \quad \text{at } K=0$$

$$W=\sqrt{2}, \quad W' = 1/\sqrt{2} \quad \text{at } K=1.$$

These are conditions that all isotropic dispersion equations satisfy.

The performance of this approximation for isotropic aluminum is illustrated in Figs. 3. It can be seen that in the range  $K=0 \sim 1$ , the approximation does a very good job over all, even for  $W''$ . Similar approximations for isotropic copper and steel were also examined and found to work satisfactory. With the approximate dispersion equation,  $d\omega/dk$  and

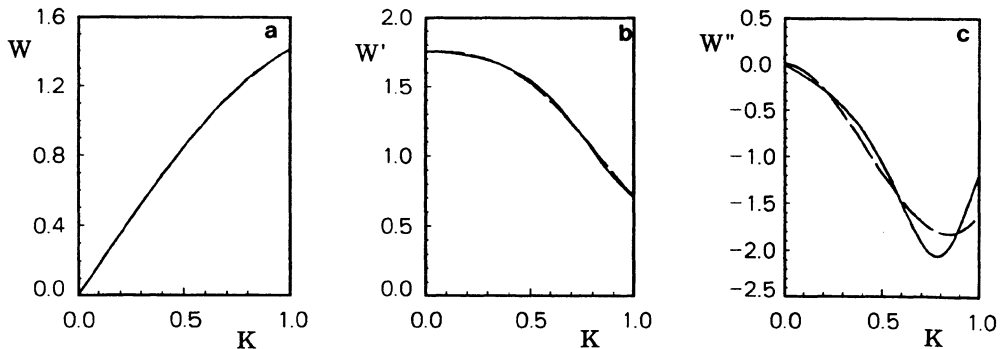


Fig.3. Approximation of dispersion curves (a)  $W(K)$ , (b)  $W'(K)$ , (c)  $W''(K)$ , (— exact, ---- approximated)

$d^2\omega/dk^2$  can be easily obtained. Thus,  $V_g=d\omega/dk=V_t dW/dK$  and  $\omega''=d^2\omega/dk^2=(b/\pi) V_t d^2W/dK^2$ .

Using Eqs. (3) and (4), some computer simulations were made to determine the detailed effects of dispersion on phase shift and velocity measurements. Let us define the relative error as  $(V_m-V_p)/V_p$ , where  $V_m$  is the measured velocity and  $V_p$  is true phase velocity. In addition to the plate thickness, this error is determined by the following variables:  $x$ , the transducer separation distances;  $D$ , the EMAT period;  $\nu$ , the Poisson ratio; and  $B$ , the pulse width at the beginning of propagation.

Figs. 4-7 are simulations of the relative error when one tracks the zero crossing initially having zero excess phase (Eq. 3b) at  $x=0$ . This cycle is initially at the center of the packet but moves away from the center as the pulse propagates. In (a) of Figs. 4-7, relative errors are plotted vs. thickness  $b$  of the plate. In (b) of Figs. 4-7, relative amplitude of measured zero-crossing  $(A_g-A_m)/A_g$  are plotted, where  $A_m$  is the magnitude (usually in volts) of the signal envelope at the measured zero-crossing time, and  $A_g$  is the magnitude of the maximum signal (peak voltage) or envelope magnitude at the time of  $t=x/V_g$ . Table I shows the fixed and varied parameters which are used in Figs. 4-7. The fixed values selected here for simulation are based on the set-up at our laboratory. Keep in mind that the relative amplitude plots give an indication regarding whether the zero-crossing is in the pulse envelope. In practice, the selected zero-crossing is the one adjacent to the peak with maximum amplitude in the pulse; this zero-crossing may or may not have zero excess phase at the beginning of propagation depending on the plate thickness. In experiment, when  $(A_g-A_m)/A_g$  exceeds 0.5, the measured time delay is usually not reliable because of poor signal to noise ratio.

From Figs. 4, one sees that the error is generally less than  $1 \times 10^{-3}$  for  $b < 2$  mm. For thicker plates, the dispersion effects become stronger and the errors increase rapidly after a flat region. As the separation of transducers becomes larger, the flat region becomes shorter. Notice that, however, when the error begins to increase rapidly, the corresponding zero-crossing also begins to move out of the pulse envelope. From Figs. 5, one sees how pulse width influences the relative error. The narrower the pulse width, the smaller the plate thickness must be to avoid introduction of large error in the measurement process. Figs. 6 shows the effects of another parameter  $D$ , the EMAT's period on the measurement error. It is demonstrated that the period of EMATs (hence the wave number  $k$ ) has a very important role in the pulse distortion. This of course can be interpreted from the  $S_0$  dispersion curve. For small  $kb$  or  $b/D$ , the dispersion is not severe. As  $kb$  increases (due to decrease in  $D$ ), the dispersion becomes strong, thus introduces more error. Figs. 7 display the effects of Poisson's ratio on the measurement error. It seems that Poisson's ratio has a very limited influence on the error curves, even though the range of Poisson's ratio in the figures covers a wide range of engineering materials.

To ascertain how much error is introduced if the velocity is determined

Table I. Fixed and variable parameters in Figs. 4-7.

| Fig. | $x(\text{mm})$ | $D(\text{mm})$ | $\nu$ | $B(\text{mm})$ |
|------|----------------|----------------|-------|----------------|
| 4    | vary           | 10.0           | 0.345 | 20.0           |
| 5    | 150.0          | vary           | 0.345 | 20.0           |
| 6    | 150.0          | 10.0           | vary  | 20.0           |
| 7    | 150.0          | 10.0           | 0.345 | vary           |

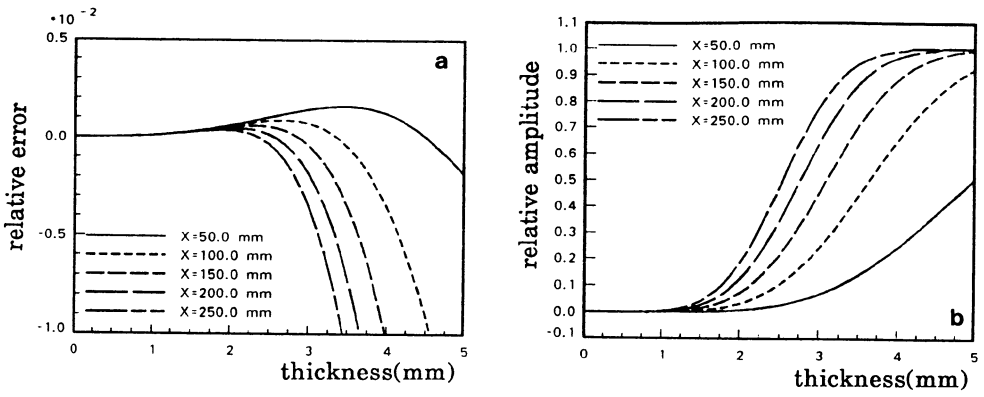


Fig.4. Effects of transducer separation distance (a) relative error vs. thickness, (b) relative amplitude vs. thickness

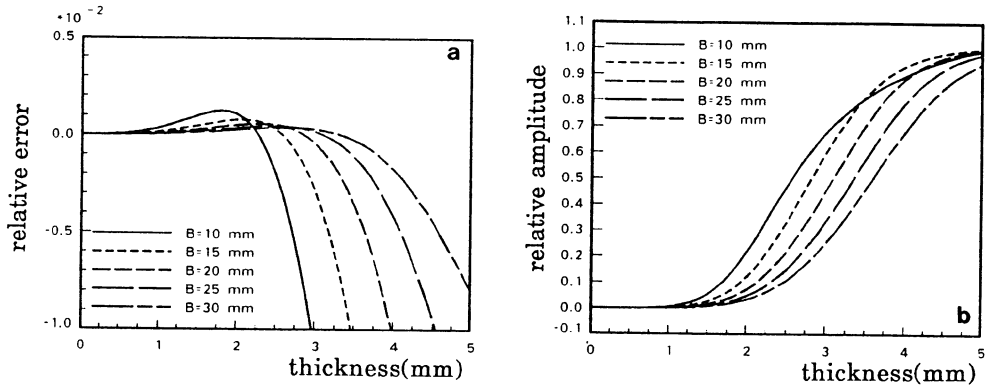


Fig.5. Effects of transducer period, (a) relative error vs. thickness, (b) relative amplitude vs. thickness

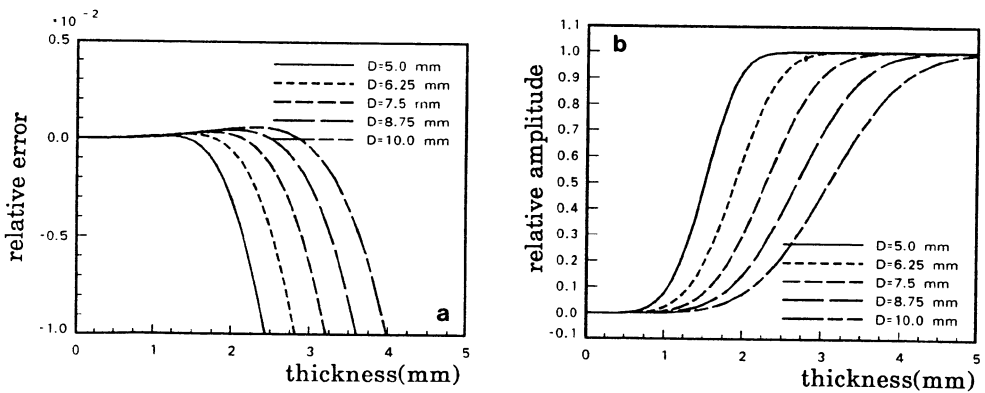


Fig.6. Effects of Poisson's ratio of material (a) relative error vs. thickness, (b) relative amplitude vs. thickness

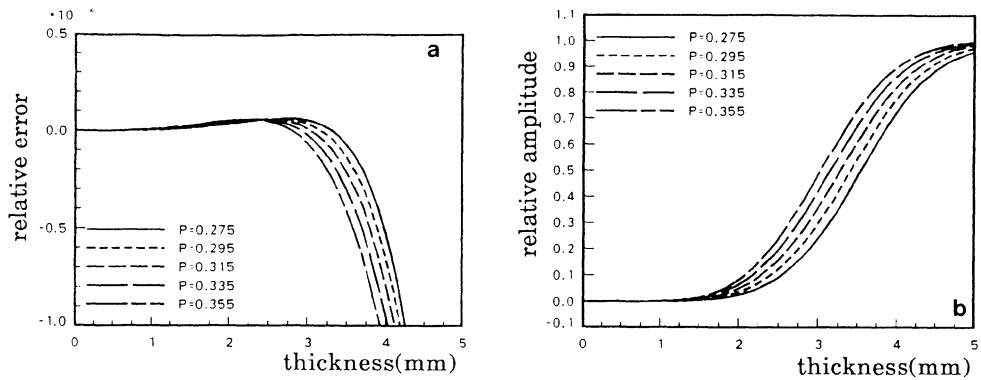


Fig.7. Effects of pulse width of wave (a) relative error vs. thickness, (b) relative amplitude vs. thickness

by the slope of  $t-x$  plot, we plotted  $(V_r - V_p)/V_p$  vs. thickness in Fig. 8(a), where  $V_r$  is the velocity obtained through linear regression of time delay and transducer separation distances. Each velocity is computed from eleven separations (200–300 mm by 10 mm). In Fig. 8(b), the average relative amplitudes, which is defined as the mean of relative amplitudes at the eleven separations, are also included. The parameters used here are  $D=10.0$  mm,  $\nu=0.345$ , and  $B=20.0$  mm. There are ten curves in Figs. 8, corresponding to ten zero-crossings. The ten zero-crossings have phase  $\phi=2n\pi$  ( $n=0\sim 9$ ) at  $x=0$  and  $t=0$ . As mentioned before, the zero-crossing selected for time measurement, which is usually the one adjacent to the pulse peak, does not necessarily have zero initial phase ( $\phi=0$ ). If one uses the average relative amplitude as a discriminant, one can see that for plates of thickness less than 1.5 mm, the zero-crossing with zero initial phase ( $n=0$ ) is most likely to be selected for the time measurement; for plates of thickness  $b=1.5\sim 2.0$  mm, the zero-crossing with phase  $\phi=2\pi$  ( $n=1$ ) is most likely to be selected, etc.

To see clear how much error is produced, we plotted the part of Figs. 8 that has practical significance in Figs. 9 and used different vertical scales. Fig. 9(a) shows only the error curve for the zero-crossings with minimum average relative amplitudes. It can be readily seen that the velocity error is generally bounded within  $\pm 2.0 \times 10^{-3}$ , an acceptable measurement error in texture characterization for plate thickness of less than 4 mm. Note the error fluctuates when thickness goes over 2 mm. This indicates that the exact error may be difficult to predict for thicker plates.

## CONCLUSION

The pulse distortion and phase shift for a pulse propagation in a dispersive media are modeled and studied for a Gaussian shaped spatial envelope. It is shown that pulse spreading, skewing, and phase shift of zero-crossings are the consequences of non-zero  $\omega''$ . We have simulated the pulse distortion and phase shift effects and assessed the consequent errors in velocity measurements. It is found that this aspect of dispersion does not induce severe discrepancy in the velocity measurement of the  $S_0$  wave for the current texture experiment configuration when the plate thickness is less than 4 mm and the error tolerance  $\delta V/V$  is set to  $2.0 \times 10^{-3}$ . Hence, this aspect of dispersion may be ignored.

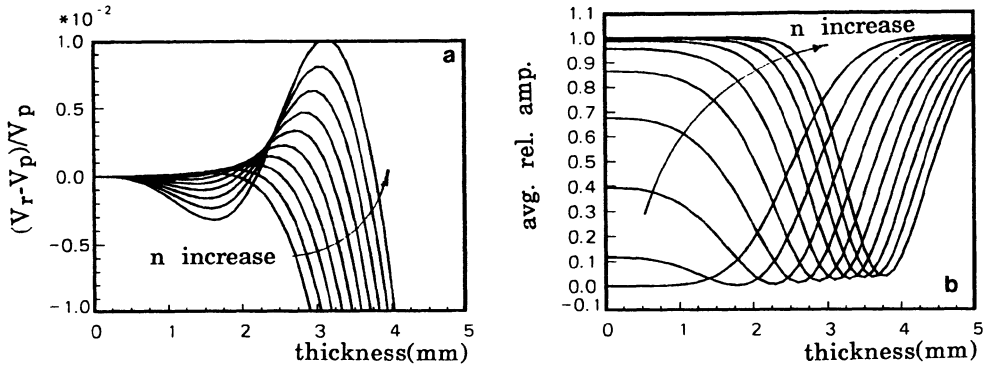


Fig.8. Error in velocity from linear regression (a) error vs. thickness, (b) relative amplitude vs. thickness

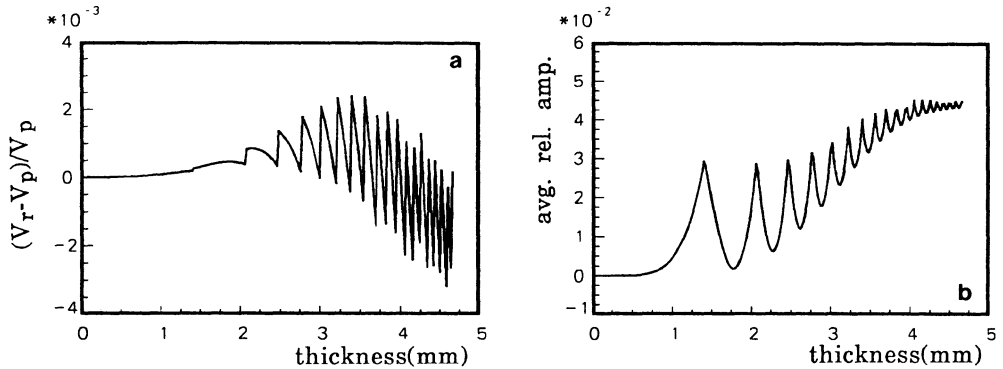


Fig.9. The part of Fig. 8 which bears practical significance.

#### ACKNOWLEDGEMENT

Ames Laboratory is operated for the U. S. Department of Energy by the Iowa State University under contract No. W-7405-Eng-82. This work was supported by the Director for Energy Research, Office of Basic Energy Sciences.

#### REFERENCES

1. R. B. Thompson, S. S. Lee, and J. F. Smith, *Ultrasonics* 25, 133 (1987).
2. R. B. Thompson, J. F. Smith, S. S. Lee, and G. C. Johnson, "A Comparison of Ultrasonic and X-ray determinations of Texture in Thin Cu and Al plates", *Met. Trans.* in press.
3. R. B. Thompson and R. K. Elsley, "A Prototype EMAT System for Inspection of Steam Generator Tubing", report for Research Project S101-1, EPRI NP-2836, 1983 (Electric Power Research Institute, Palo Alto, California).